ARTICLE IN PRESS

Available online at www.sciencedirect.com

ScienceDirect

Chemie der Erde ▮ (▮▮▮▮) ▮▮▮–▮▮▮

CHEMIE der ERDE GEOCHEMISTRY

www.elsevier.de/chemer

Late Neoproterozoic A-type granites in the northernmost Arabian-Nubian Shield formed by fractionation of basaltic melts

G.H. Jarrar[a,*], W.I. Manton[b], R.J. Stern[b], D. Zachmann[c]

[a]*Department of Applied and Environmental Geology, University of Jordan, P.O. Box 13633, Amman 11942, Jordan*
[b]*Geosciences Department, University of Texas at Dallas, P.O. Box 830688, USA*
[c]*Institute für Umweltgeologie, Pockelsstr. 3, Braunschweig 38 106, Germany*

Received 20 February 2006; accepted 12 September 2006

Abstract

Geochemical, isotopic and age constraints support a comagmatic origin for Ghuweir Mafics and the Feinan A-type granites. The two rocks types, named collectively in this paper as the Feinan Ghuweir Magmatic Suite (FGMS), formed between 556 and 572 Ma ago according to Rb–Sr whole-rock dating. FGMS has low Sr initial ratios, which preclude a significant contribution of much older crust in the magma genesis.

The FGMS has a wide range of silica contents, with a gap at 55–65 wt% SiO_2. It has a transalkaline to alkaline character; belongs to the medium to high K calc-alkaline series; it ranges from metaluminous to mildly peraluminous character and belongs to the alkali and alkali-calcic series. The Feinan granites and the Ghuweir rhyolites and rhyodacites are classified as A-type granites and belong to group A2 of Eby [Eby, N.G., 1992. Chemical subdivision of the A-type granitoids: petrogenetic and tectonic iplications. Geology 20, 641–644].

According to geochemical modeling the Ghuweir Mafics were derived from a subduction modified lithospheric mantle by 10% batch modal partial melting of a phlogopite-bearing spinel lherzolite. The intra-suite geochemical variations can be ascribed to fractional crystallization of olivine, pyroxene, and plagioclase. The accumulation of apatite in the most evolved samples is responsible for the high concentrations of REE.

The Feinan granites and the Ghuweir rhyolites and rhyodacites were derived from the mafic magma by the fractional crystallization of ≈78% of the original magma to the mineral assemblage olivine + pyroxene + plagioclase + magnetite. The intra-suite geochemical variations in the Feinan A-type granites are due to the fractional crystallization of the mineral phases: amphibole + Na and K-feldspar + apatite + magnetite + zircon + allanite.

The FGMS correlates with time-equivalent rocks in many parts of the Arabian-Nubian Shield and the surrounding areas.

Keywords: Arabian-Nubian Shield; Jordan; Mafic magma; A-type granite; Geochronology

1. Introduction

The Arabian-Nubian Shield (ANS) is a Neoproterozoic tract of juvenile crust (Stoesser and Camp, 1985). The ANS formed during the Pan-African Orogeny

*Corresponding author. Fax: +962 6 5348932.
E-mail address: jarrargh@ju.edu.jo (G.H. Jarrar).

0009-2819/$ - see front matter © 2006 Elsevier GmbH. All rights reserved.
doi:10.1016/j.chemer.2006.09.002

Please cite this article as: Jarrar, G., et al., Late Neoproterozoic A-type granites in the northernmost Arabian-Nubian Shield formed by fractionation of basaltic melts. Chemie der Erde (2006), doi:10.1016/j.chemer.2006.09.002

(ca. 900−550 Ma) by amalgamation of arc terranes, which was followed by the intrusion of vast volumes of granitoids of calc-alkaline character (e.g. Stoesser and Camp, 1985). It is known for the abundance of 'A'- type Neoproterozoic granites described by Sylvester (1989) as typical post-collisional alkaline granites.

Greiling et al. (1994) and Beyth et al. (1994) emphasized that the collisional phase terminated at ~615−600 Ma and subsequent structural collapse occurred only within the 595−575 Ma time span and was followed by transpressional tectonism along major shear zones.

The final phase of the Neoproterozoic Pan-African Orogeny witnessed widespread magmatism of bimodal, alkaline and transitional character around 600−550 Ma (e.g. Stern and Gottfried, 1986; Jarrar et al., 1992). A-type granites and coeval mafic magmas (monzogabbros, monzodiorites and their volcanic equivalents) form an essential part of this phase.

Several petrogenetic schemes have been proposed for the origin of A-type granites; nevertheless, the most widely discussed models fall into two broad categories: (1) as fractionation products of mantle-derived mafic magmas (Collins et al., 1982; Turner et al., 1992; Beyth et al., 1994); (2) as anatectic melts of lower crustal rocks (Creaser et al., 1991; Landenberger and Collins, 1996; King et al., 1997). The existence of both mantle- and crustal-derived A-type granites has also been advocated (Eby, 1992).

In this investigation, the petrogenesis of Feinan A-type Granite is discussed in terms of the first model, i.e. as a fractionation product of the consanguineous Ghuweir Mafics on the basis of new field, petrographic, geochemical, and isotopic data.

2. Geological setting and previous work

The study area is located in central Wadi Araba, about 130 km north of the Gulf of Aqaba, among the northernmost exposures of the Arabian-Nubian Shield (Fig. 1). This Neoproterozoic basement has been divided into two major lithostratigraphic divisions separated by a regional Late Neoproterozoic unconformity; namely the older Aqaba complex and the younger Araba complex (e.g. Ibrahim and McCourt, 1995). This unconformity has been placed at about 600 Ma in Jordan and the adjacent countries (Hadley and Schmidt, 1980; Bentor, 1985; Willis et al., 1988; Jarrar et al., 1993). This unconformity is marked by the onset of intermontane molasse sediment deposition (Hammamat series in the northeastern desert of Egypt; Shammar group in Saudi Arabia; Saramuj Conglomerate in Jordan). The Araba Complex includes all rocks post-dating this unconformity. Since the Ghuweir Mafics intrude Saramuj-type sediments in Wadi Ghuweir (this study) and are dated at 573 Ma (see age constraints) they seem to be contemporaneous with the sediments of the Araba complex which suggest that the Araba complex in the area of study comprises two lithologies, which are associated in space and time and were previously defined as the Ghuweir Porphyrites and the Feinan Granite.

3. Field and petrographic aspects

3.1. Ghuweir Mafics

The mafic part of the investigated suite is collectively known as Ghuweir Volcanics (Basta et al., 1982; Al-Bakri, 1990). It should however, be emphasized that these overwhelmingly basaltic to andesitic rocks intrude Saramuj-type sediments, in contrast to what has been suggested by previous authors; namely, that the Saramuj-type sediments overly the Ghuweir Volcanics. Therefore, these rocks are renamed as the *Ghuweir Mafics* and will be referred to hereafter as *GM*. The Saramuj-type clastic sediments attain a thickness of up to 30 m and were brought to steep dip (up to 60°) during the very shallow emplacement of the GM as demonstrated by the minimal thermal effects on the sediments. Xenoliths from the Saramuj-type clastics are present in the mafics directly at the contact. The GM consist primarily of plagioclase, augite, and pseudomorphs after olivine in the basaltic samples, and titanomagnetite; chlorite and epidote are abundant secondary phases. Plagioclase is present as phenocrysts (up to 3 mm across) and as a principal constituent of the groundmass (0.1×0.5 mm laths). The two samples (GW-22, -23; Table 2) with the most primitive composition, i.e. Mg # of 61 and 59, are microgabbros consisting of large ophitic augite grains enclosing tabular plagioclase laths, olivine pseudomorphs and titanomagnetite.

The GMs are cut by NE trending, up to 5 m thick rhyolite and rhyodacite dikes. These dikes are fine-grained and contain sparse phenocrysts of sanidine in a groundmass of alkali feldspar and quartz with accessory opaques, apatite, and rare secondary chlorite. These dikes do not cut the Feinan granite (see below) and will be referred to hereafter as *Ghuweir Rhyolites* (*GR*).

3.2. Feinan granite (FG)

The contact of the FGs with the GMs is tectonic. The FG is commonly pink due to abundant brick red alkali feldspar. In addition to quartz accessories of oxides, zircon, biotite, titanite, aegirine, amphibole, apatite and fluorite are present. Hornblende, aegirine and fluorite were only observed in two samples. Perthite, both patch- and microperthitic, are dominant in most samples and

Please cite this article as: Jarrar, G., et al., Late Neoproterozoic A-type granites in the northernmost Arabian-Nubian Shield formed by fractionation of basaltic melts. Chemie der Erde (2006), doi:10.1016/j.chemer.2006.09.002

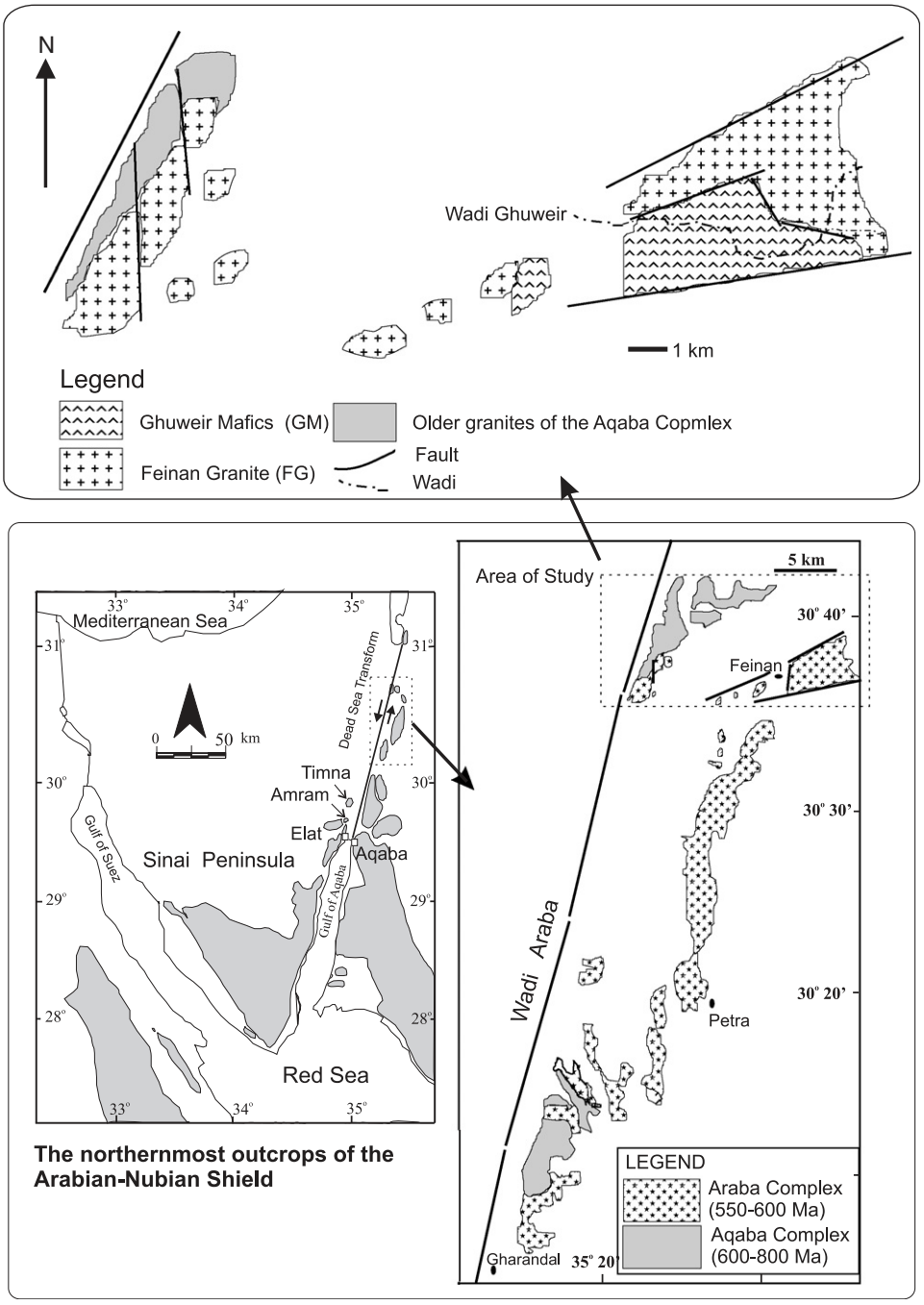

Fig. 1. Geological sketch maps with location of the investigated magmatic suite in relation to the major lithostratigraphic units of the basement complex in Wadi Araba, SW Jordan.

occurring as grains up to 6 mm across. Discrete equant grains of albite are also present, but never exceed 10% of the whole rock. Quartz is the second major constituent and occurs as anhedral grains up to 5 mm across. The modal abundance of quartz is as high as 40%, which is reflected in the high silica content of the granites (up to 81 wt%). Micrographic intergrowth of quartz and microperthite is common and dominant in some samples. To conclude, FG is mainly a hypersolvus high silica granite; though low silica varieties are present but never widespread (GW-34). The three igneous rock suites (GM,GR, FG) will be referred to hereafter as the Feinan Ghuweir Magmatic Suite (*FGMS*).

4. Analytical techniques

Major and trace elements for 30 samples from the FGs and GMs and rhyolite/rhyodacite dikes were

Please cite this article as: Jarrar, G., et al., Late Neoproterozoic A-type granites in the northernmost Arabian-Nubian Shield formed by fractionation of basaltic melts. Chemie der Erde (2006), doi:10.1016/j.chemer.2006.09.002

determined at the Chemex Labs, Reno, NV, USA and at the Institute for Environmental Geology of the Technical University of Braunschweig, Germany. The major oxides including Cr_2O_3 were analyzed by meta-borate fusion ICP-OES technique while the trace elements including REE were determined by Inductively Coupled Plasma-Mass Spectrometry (ICP-MS) techniques. Replicate analyses indicate a reproducibility of better than 2% and 5% for major and trace elements, respectively.

The Rb, Sr, Sm, and Nd concentrations for whole-rock samples were determined by isotope dilution at the Geosciences Department, University of Texas at Dallas, USA.

Analytical procedures are detailed in Stern et al. (1994). The analyses were carried out on the UTD Finnigan MAT 261 instrument. During the course of the study the value obtained for the $^{87}Sr/^{86}Sr$ ratio of the NBS 987 standard averaged 0.710264 ± 0.000012 (2σ) while the average value of 0.511861 ± 0.000006 (2σ) was obtained for the $^{143}Nd/^{144}Nd$ ratio for the UCSD standard.

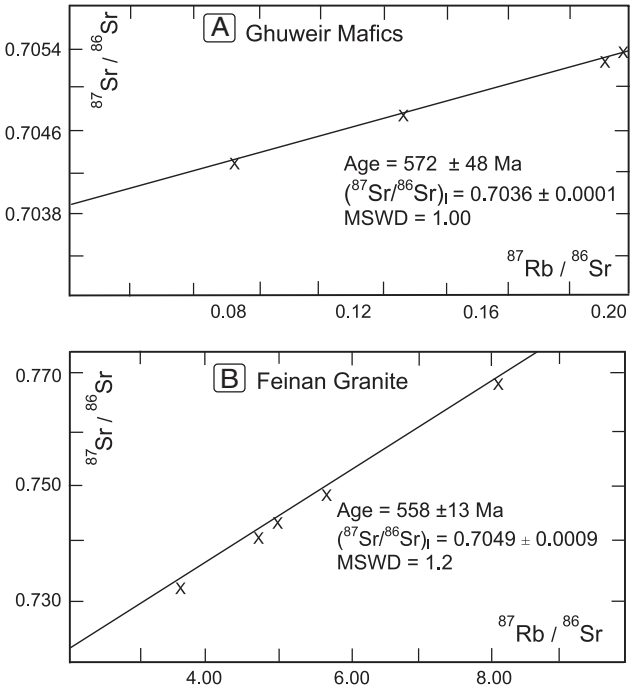

Fig. 2. Rb-Sr isochrons for: (A) Ghuweir mafics; (B) Feinan Granites.

5. Age constraints

The Rb–Sr whole-rock technique was applied to obtain age constraints on the GMs and the FG. For the strontium isochron calculation uncertainties of 0.05 for $^{87}Sr/^{86}Sr$ and 1% for $^{87}Rb/^{86}Sr$ were assumed on the basis of the reproducibility of the standard. The program ISOPLOT 3 (Ludwig 2003) was used for isochron plotting and age calculations (Fig. 2). The results of isotopic analyses are given in Table 1.

The analyzed samples from the GM define an isochron which gives an age of 572 ± 48 Ma and initial $(^{87}Sr/^{86}Sr) = 0.7036 \pm 0.0001$ (MSWD = 1.00). This age is, within error, identical to the K–Ar age of 542 ± 8 Ma reported for a latite sample from the GMs (Lenz et al., 1972). Since these mafics intrude the Saramuj type sediments, which post-date the intra-Precambrian Unconformity set at about 600 Ma (e.g. Jarrar et al., 1993) the age of 573 Ma seems reasonable. Jarrar (1985) reported two U–Pb zircon ages of 570–580 Ma for a quartz monzodiorite from Wadi Um Rachel, Central Wadi Araba. The GMs are most probably coeval to these monzodiorites.

The Rb/Sr data on five FG whole-rocks have been used to construct an isochron, from which an age of 558 ± 13 Ma and the initial $(^{87}Sr/^{86}Sr)$ ratio of 0.7049 ± 0.0009 were obtained and an MSWD of 1.20. This age is, within error, also similar to the Rb–Sr date (538 ± 30 Ma) obtained by Brook et al. (1990) for the FG, and similar to ages obtained for the geochemically similar Humrat and Mubarak granites East and NE of Aqaba. Brook et al. (1990) obtained Whole-Rock Rb–Sr ages at 567 ± 5 Ma and 560 ± 10 Ma for the above two granites, respectively. We tend even to constrain the age of FG between 555 and 570 Ma. Taking the uncertainties in the isochron calculation into account, it is safe to consider the GM and FG consanguineous.

The Sm–Nd isotopic data for two samples from the GM and three samples from the FG are listed in Table 1. The average $\varepsilon_{Nd(t)}$ and T_{DM} are +4.0, +4.3 and 0.81, 0.77 Ga for the GM and FG, respectively. The similarity of $\varepsilon_{Nd(t)}$ values can be taken as a further support for the hypothesis that the GM and FG are comagmatic. The difference of only 200 Ma between the Rb/Sr ages and model ages T_{DM} cannot be explained in terms of contamination with crustal material older than the Pan-African.

The low initial $(^{87}Sr/^{86}Sr)$ values for the GM is evidence for a mantle derivation of these mafics. Even the initial values for the FG are too low to infer a significant Pre-Pan African crustal contribution in the formation of the FG.

6. Geochemistry

The database used in this study consists of major and trace elements for 30 samples from the FG, the GMs and Ghuweir rhyolites and rhyodacites (GR) (Table 2). The FGMS forms a discontinuous compositional spectrum of 48–81% SiO_2, with a gap at 55–65% SiO_2

Please cite this article as: Jarrar, G., et al., Late Neoproterozoic A-type granites in the northernmost Arabian-Nubian Shield formed by fractionation of basaltic melts. Chemie der Erde (2006), doi:10.1016/j.chemer.2006.09.002

Table 1. Rb–Sr and Sm–Nd isotopic data for the Ghuweir Mafics and Feinan Granites together with the calculated ages, initial ratios and other relevant isotopic parameters

Sample	Lithology	Rb (ppm)	Sr (ppm)	$^{87}Rb/^{86}Sr$	$^{87}Sr/^{86}Sr$		
Feinan granite (FG)							
GW-25	Granite	116.2	48.02	7.9025	0.768052	Age = 558 ± 23 Ma	
GW-28	Granite	121.5	44.9	4.774	0.742764	$(^{87}Sr/^{86}Sr)_I = 0.7049 \pm 0.0009$	
87/54	Granite	132	70	5.492	0.748210	MSWD = 1.20	
87/56	Granite	127	81	4.546	0.741320		
87/60	Granite	124	105	3.427	0.732265		
Ghuweir Mafics (GM)							
GW-4	Basalt	42.2	822.2	0.14224	0.70472	Age = 572 ± 48 Ma	
GW-8	Basaltic andesite	64.8	876.3	0.20708	0.70521	$(^{87}Sr/^{86}Sr)_I = 0.7036 \pm 0.0001$	
GW-19	Trachybasalt	46.8	627.6	0.21185	0.70532	MSWD = 1.00	
GW-21	Basaltic trachandesite	14.8	451.9	0.08989	0.70429		
		Sm (ppm)	Nd (ppm)	$^{147}Sm/^{144}Nd$	$^{143}Nd/^{144}Nd$	$\varepsilon Nd(t)$	TDM (Ga)
Sm–Nd isotopic data							
GW-19	Trachybasalt	9.11	44.7	0.123182	0.512556	+3.77*	0.83
GW-21	Basaltic trachandesite	9.7	49.6	0.118392	0.512561	+4.23*	0.78
GW-25	Granite	4.5	27	0.101067	0.512530	+4.74**	0.71
GW-32	Granite	6.6	42.4	0.093832	0.512473	+4.14**	0.73
GW-35	Granite	3.9	16.4	0.144643	0.512654	+4.04**	0.87

ε.Nd(t) are calculated using the following ages. * = 572 Ma; ** = 556 Ma.The errors are 0.00001 in Sr/Sr ratios and 0.000006 in Nd/Nd ratios as 2σ.

(Fig. 3A). The FGMS plots on the boundary between the alkaline and subalkaline fields on the TAS diagram (Fig. 3A) as defined by various authors (Irvine and Baragar, 1971; Mcdonald and Katsura, 1964). If the dividing line of Miyashiro (1978) is applied, the whole suite falls into the alkaline field. Therefore, we selected the most recent divider (Middlemost, 1997) since it divides the TAS space into alkaline, transalkaline (midalkaline) and subalkaline (calcalkaline and tholeiitic) fields. The great majority of the FGMS plots the transalkaline field (Fig. 3A). Furthermore, the GM plots in the fields of basalt, trachybasalt, basaltic trachyandesite and basaltic andesite; while FG falls exclusively in the field of granites but one FG sample together with the GR falls in the trachydacite field very close to the dacite field. Few samples of GM and FG plot at the boundary to the sub-alkaline field. In the K_2O vs. SiO_2 diagram of Rickwood (1989), the GM extend from the medium K- through high K calc-alkaline to the shoshonitic series (diagram not shown). The GR plot in the shoshonite and high-K fields while the FG are restricted to the high-K series. The investigated rocks are plotted on Shand's index (Maniar and Piccoli, 1989) classification diagram (Fig. 3B). The GM is metaluminous, while the FG and GR are metaluminous to mildly peraluminous (A/CNK > 1). Most of FG samples contain minor normative corundum (0.4–1.85 wt%). On the Peacock diagram (Brown, 1981), the FGMS follows a trend from alkalic to alkali-calcic (Fig. 3C). GMs contain zero to 10 wt% normative quartz and none of the analyzed rocks contain normative nepheline. When plotted on K_2O/Na_2O vs. SiO_2 diagram (not shown), the FGMS shows a progressive increase of K_2O/Na_2O with increasing silica.

Harker type variation diagrams of silica vs. major and trace elements are shown in Fig. 4. The plot of Al_2O_3 vs. SiO_2 shows an increasing trend until 55% silica, after which Al_2O_3 decreases due to the onset of plagioclase fractionation. FeO, MgO (not shown) and CaO decrease with increasing silica, which reflects the separation of olivine, magnetite, pyroxenes, and plagioclase. Sr, TiO_2, Y, and Zr display bell-shaped trends for the GM and FG, respectively. These elements behave incompatibly during the evolution of the GM, and compatibly during the fractionation of the GR and FG. Ni decreases from 175 ppm at Mg# = 61 to 10 ppm at Mg# = 44 reflecting an important role of olivine separation in the evolution of the GM. Rb and K increase from the GM through GR and FG sub-suites.

The FG and GR are plotted on a series of diagrams designed by Whalen et al. (1987) to discriminate A-type granites (Fig. 5) These granites plot either in the field of A-type granites, or close to the boundary of the A-type granites on the Ga/Al vs. (Zr + Y + Nb + Ce) and $(Na_2O + K_2O)/CaO$ plots. Furthermore, the GR and FG fall in the A_2 subtype of Eby (1992) on the Nb–Rb/Nb vs. Y/Nb plot (Fig. 5), which Eby interpreted as anatectic melts from continental crust.

The FG rocks have moderate REE abundances ($\sum$REE = 113–261 ppm) (Table 2, Fig. 6A) and are

Please cite this article as: Jarrar, G., et al., Late Neoproterozoic A-type granites in the northernmost Arabian-Nubian Shield formed by fractionation of basaltic melts. Chemie der Erde (2006), doi:10.1016/j.chemer.2006.09.002

Table 2. Major (in wt%) and trace (in ppm) element concentrations and elemental ratios for the investigated FGMS

	Ghuweir Mafics													
	GW4	GW5	GW6	GW7	GW8	GW11	GW12	GW14	GW18	GW19	GW21	GW22	GW23	GW24
SiO_2	52	49.92	54.2	54	52.98	51.5	51	52.39	52.52	50	53.23	49	48	52
TiO_2	1.65	2.46	1.51	1.63	1.57	1.52	2.46	1.66	1.79	1.93	1.72	1.22	1.13	1.58
Al_2O_3	15.84	14.97	15.48	15.82	15.43	15.97	14.12	16.01	15.26	16.05	15.06	14.86	14.92	16.12
Fe_2O_3	9.02	11.2	8.62	8.92	8.51	8.88	11.25	9.01	9.3	10.72	8.44	11.83	11.6	9.28
MnO	0.12	0.17	0.15	0.15	0.16	0.13	0.15	0.12	0.11	0.14	0.11	0.14	0.17	0.13
MgO	5.67	4.91	5.16	5.69	5.22	5.75	4.39	5.66	5.94	6.16	4	8.44	8.98	6.07
CaO	5.92	5.92	6.08	5.29	6.25	6.18	5.62	5.51	4.21	4.46	5.73	8.49	8.54	3.78
Na_2O	2.68	3.59	2.68	4.53	3.09	2.72	3.15	3.21	4.68	4.93	6.21	2.39	2.42	4.67
K_2O	1.52	2.48	2.13	1.23	1.86	2.02	2.42	1.87	2.13	1.68	0.76	0.82	1.05	1.65
P_2O_5	0.81	0.93	0.67	0.72	0.72	0.59	1.35	0.82	0.59	0.64	0.79	0.15	0.13	0.55
LOI	4.22	3.17	2.39	2.53	2.44	5.04	4.2	4.21	3.85	3.6	4.77	3.31	3.77	4.17
Σ	99.45	99.72	99.07	100.5	98.23	100.3	100.1	100.5	100.4	100.3	100.8	100.7	100.7	100
Mg#	55	46	54	56	55	56	44	55	56	53	48	59	61	56
Cs	3.7	6.3	3.4	1.2	3.7	3	2.6	4.6	0.5	0.4	0.1	1.2	1.8	0.9
Rb	42.2	85	73.8	38.4	64.8	66.2	65.8	53.4	48	46.8	14.8	17.2	22.8	43
Ba	824	844	1300	534	1095	796	1175	736	724	741	318	235	208	511
Sr	763	765	681	618	818	636	497	777	625	573	421	316	384	376
Pb	25	5	15	15	20	15	15	15	15	10	5	5	5	20
U	1	1	1.5	1.5	1.5	1.5	1.5	1	0.5	0.5	0.5	0	0	1.5
Th	4	4	6	5	5	6	5	4	4	3	4	1	1	4
Zr	240	295	245	237	246	226	180	240	228	233	240	104	92	193
Hf	5	7	6	5	6	5	4	5	5	5	5	3	2	5
Nb	11	22	12	11	11	11	25	11	12	14	12	5	4	9
Y	29	40	29	28	30	27	44	27	28.5	28.5	27.5	18.5	17.5	25.5
La	43	50.5	39	39	39	35	61.5	40	33.5	35.5	37.5	10.5	9.5	31
Ce	96	113.5	85.5	86	89.5	76.5	141	90.5	76.5	81	87.5	24.5	22	69
Pr	12.4	14.1	10.9	10.7	11	9.9	18	11.9	9.3	10.1	11.5	3.3	3	9
Nd	50	61	45	44.5	49	41	77.5	48.5	39	42.5	50	14.5	13.5	38.5
Sm	9.1	11.8	8.8	9.1	8.8	7.7	13.8	8.8	7.6	8.1	8.9	3.1	3.3	8.1
Eu	2.5	3	2.3	2.2	2.4	2.2	3.8	2.4	2.2	2.3	2.3	1.1	1.1	2.4
Gd	8.5	10.9	8.2	7.7	8.2	6.8	12.2	7.5	6.9	7.7	7.8	3.9	3.6	6.9
Tb	1.1	1.5	1	1.1	1.1	1.1	1.7	1.1	1	1.1	1.1	0.6	0.5	0.9
Dy	5.3	7.6	5.1	5.1	4.8	4.7	8.3	5.1	4.9	5.5	5.2	3.3	3	4.5
Ho	1	1.4	1	0.9	1.1	0.9	1.7	1	1	1	1	0.7	0.6	0.9
Er	2.5	3.9	2.5	2.4	2.8	2.6	4.2	2.5	2.7	2.5	2.7	1.8	1.6	2.2
Tm	0.3	0.5	0.4	0.3	0.3	0.3	0.6	0.3	0.4	0.4	0.3	0.3	0.2	0.3
Yb	2.3	3.5	2.5	2.5	2.3	2.2	3.5	2.3	2	2.3	2.2	1.9	1.6	2.1
Lu	0.3	0.5	0.4	0.4	0.4	0.3	0.5	0.4	0.4	0.3	0.4	0.2	0.2	0.3
REE	234.3	283.7	212.6	211.9	220.7	191.2	348.3	222.3	187.4	200.3	218.4	69.7	63.7	176.1
V	165	245	150	155	160	165	210	170	185	185	170	190	185	185
Cr	68	bdl	68	68	68	68	bdl	136	168	68	68	274	274	68
Ni	65	25	50	50	55	60	10	70	60	60	70	170	175	55
Cu	40	35	160	30	170	40	30	45	35	40	75	80	65	55
Sn	1	2	1	1	1	1	2	1	1	1	1	bdl	1	1
Zn	120	130	145	135	195	90	135	130	95	110	115	85	90	115
Ga	20	21	19	19	20	19	21	19	19	20	18	19	18	20
Ba/La	19.2	16.7	33.3	13.7	28.1	22.7	19.1	18.4	21.6	20.9	8.5	22.4	21.9	16.5
La/Yb	18.7	14.4	15.6	15.6	17	15.9	17.6	17.4	16.8	15.4	17	5.5	5.9	14.8
K/Rb	299	242	239	266	238	253	305	291	368	298	426	396	382	318
K/Ba	15	24	14	19	14	21	17	21	24	19	20	29	42	27
Rb/Sr	0.06	0.11	0.11	0.06	0.08	0.1	0.13	0.07	0.08	0.08	0.04	0.05	0.06	0.11
Ba/Zr	3.4	2.9	5.3	2.3	4.5	3.5	6.5	3.1	3.2	3.2	1.3	2.3	2.3	2.6
Th/U	4	4	4	3.3	3.3	4	3.3	4	8	6	8	0	0	2.7
Zr/Hf	48	42	41	47	41	45	45	48	46	47	48	35	46	39
Zr/Nb	22	13	20	22	22	21	7	22	19	17	20	21	23	21
Y/Nb	2.6	1.8	2.4	2.5	2.7	2.5	1.8	2.5	2.4	2	2.3	3.7	4.4	2.8

Please cite this article as: Jarrar, G., et al., Late Neoproterozoic A-type granites in the northernmost Arabian-Nubian Shield formed by fractionation of basaltic melts. Chemie der Erde (2006), doi:10.1016/j.chemer.2006.09.002

Table 2. (*Continued*)

Ghuweir Rhyolites			Feinan Granites												
GW10	GW13	GW20	GW25	GW26	GW27	GW28	GW29	GW30	GW31	GW32	GW33	GW34	GW35	GW36	GW37
65.91	66.57	70	80.5	79.69	78.59	77	76	75	77	75	74.8	68	78	77.7	75
0.84	0.87	0.57	0.07	0.08	0.09	0.15	0.21	0.22	0.14	0.18	0.27	0.42	0.05	0.12	0.23
15.33	15.05	14.49	10.42	11.48	11.79	12.42	12.94	13.33	12.6	13.36	14.07	16.42	12.75	12.73	13.42
4.5	4.14	3.46	0.89	0.93	0.9	0.93	1.27	1.34	1.03	1.46	1.63	2.72	0.73	0.98	1.38
0.07	0.04	0.05	bdl	bdl	bdl	0.05	0.04	0.05	0.03	0.04	0.06	0.09	0.02	0.04	0.03
1.34	1.32	1.05	0.08	0.06	0.05	0.15	0.26	0.27	0.24	0.2	0.25	0.86	0.06	0.16	0.26
2.02	0.94	1.02	0.14	0.24	0.18	0.41	0.38	0.65	0.4	0.81	0.57	1.4	0.37	0.45	0.7
3.95	4.36	4.99	3.28	3.58	3.57	3.92	4.26	4.18	4.01	4.09	4.51	4.72	4.16	4.15	4.06
4.42	5.04	3.74	3.78	4.13	4.43	4.47	4.16	4.49	4.26	3.48	3.84	4.18	3.41	3.42	3.62
0.21	0.23	0.18	0.01	0.01	0.01	0.01	0.03	0.03	0.01	0.01	0.03	0.1	0.01	0.01	0.01
2.33	1.6	1.15	0.49	0.56	0.56	0.76	0.75	0.75	0.52	1.09	0.36	0.64	0.38	0.47	0.87
100.9	100.2	100.7	99.66	100.8	100.2	100.3	100.3	100.3	100.2	99.72	100.4	99.55	99.94	100.2	99.58
37	39	38	15	11	10	24	29	29	32	21	23	39	14	24	27
1.1	4.7	0.5	1.7	1.6	2.2	1.5	1.4	2.3	2.5	1.9	1.2	1.2	2.6	5.1	1.9
129	135	90.8	117	130	141.5	124	128.5	125.5	142	143	91.2	84	220	196	133
1100	1430	953	373	287	375	226	356	434	197	334	328	717	42	146	379
295	325	286	51	40	63.1	47.2	75.7	81.2	34.2	53	66	194	11.1	26	71
15	90	10	15	10	15	170	60	15	30	45	15	20	20	25	20
2.5	3.5	2	3	2.5	2.5	6	4	3	4	3.5	3	2.5	7.5	8.5	4
9	8	9	11	13	17	16	16	17	17	18	13	10	20	23	27
412	416	327	102	100	129	174	242	182	144	171	300	305	132	154	195
9	10	8	3	3	4	5	7	4	5	5	7	7	6	5	5
19	20	13	9	11	13	12	13	10	11	13	9	9	20	18	13
34	32	28.5	12	15	20	20	25	19	20	25	22	27	36	31	24
44	42.5	34.5	26	26	31	34	37	43.5	38	38.5	47	56	20.5	46	43.5
90	86	81	76.5	53.5	68	69.5	71	88	79	76	93.5	115.5	45	91.5	90
10.9	11.2	9.4	5.6	5.8	6.8	7.9	8.2	9.6	8.3	8.7	11	13.1	5	9.6	10
44.5	45.5	35.5	19.5	19	22	26	29.5	34	28.5	29	40.5	47.5	17.5	32	32.5
7.9	8.4	7	3.6	3.4	3.5	4.8	4.8	5.9	4.6	5.2	7.1	8.8	4.4	6	5.7
1.5	1.7	1.3	0.3	0.2	0.3	0.4	0.5	0.7	0.4	0.5	0.6	1.4	0.1	0.3	0.7
7.1	7.5	5.9	2.6	3	3.1	3.8	4.2	4.4	3.8	4.6	5.4	6.9	4.4	4.6	5.3
1.1	1	0.9	0.4	0.5	0.5	0.6	0.6	0.6	0.6	0.7	0.8	1	0.8	0.9	0.8
5.5	5.4	4.2	2.1	2.3	3.2	3.5	3.7	3.4	3	3.8	3.9	4.9	5.2	4.6	3.6
1.1	1.1	1	0.4	0.5	0.6	0.6	0.8	0.6	0.6	0.8	0.8	0.9	1.1	1	0.8
3	2.9	2.5	1.2	1.2	2	1.7	2.3	1.8	2.1	2.3	2	2.4	3.4	3	2.3
0.4	0.4	0.4	0.1	0.1	0.2	0.3	0.4	0.3	0.3	0.4	0.3	0.3	0.6	0.3	0.4
3	3.1	2.4	1.3	1.3	1.9	1.8	2.4	1.9	1.9	2.5	1.7	2.3	3.9	3.7	2.3
0.4	0.5	0.4	0.1	0.2	0.3	0.3	0.4	0.3	0.3	0.4	0.3	0.3	0.6	0.5	0.4
220.4	217.2	186.4	139.7	117	143.4	155.2	165.8	195	171.4	173.4	214.9	261.3	112.5	204	198.3
50	45	40	10	10	5	5	10	5	5	5	10	20	0	5	5
bdl	bdl	bdl	bdl	bdl	bdl	bdl	bdl	bdl	bdl	bdl	bdl	bdl	bdl	bdl	bdl
5	5	10	5	5	5	5	5	5	5	5	5	10	5	5	5
45	105	15	10	25	5	5	130	5	20	5	15	50	5	10	10
2	2	2	1	1	1	1	3	2	1	2	1	1	1	3	3
60	85	60	bdl	bdl	bdl	15	40	20	30	5	25	50	5	25	20
19	17	17	12	12	13	17	18	17	17	18	17	20	19	18	17
25	33.6	27.6	14.3	11	12.1	6.6	9.6	10	5.2	8.7	7	12.8	2	3.2	8.7
14.7	13.7	14.4	20	20	16.3	18.9	15.4	22.9	20	15.4	27.6	24.3	5.3	12.4	18.9
284	310	342	268	264	260	299	269	297	249	202	349	413	129	145	226
33	29	33	84	119	98	164	97	86	179	86	97	48	674	194	79
0.44	0.42	0.32	2.29	3.25	2.24	2.63	1.7	1.55	4.15	2.7	1.38	0.43	19.82	7.54	1.87
2.7	3.4	2.9	3.7	2.9	2.9	1.3	1.5	2.4	1.4	2	1.1	2.4	0.3	0.9	1.9
3.6	2.3	4.5	3.7	5.2	6.8	2.7	4	5.7	4.25	5.1	4.3	4	2.7	2.7	6.8
46	42	41	34	33	32	35	35	46	29	34	43	44	22	30.8	39
22	21	25	11	9	10	15	19	18	13	13	33	34	6.6	9	15
1.8	1.6	2.2	1.3	1.4	1.5	1.7	1.9	1.9	1.8	1.9	2.4	3	1.8	1.7	1.8

Please cite this article as: Jarrar, G., et al., Late Neoproterozoic A-type granites in the northernmost Arabian-Nubian Shield formed by fractionation of basaltic melts. Chemie der Erde (2006), doi:10.1016/j.chemer.2006.09.002

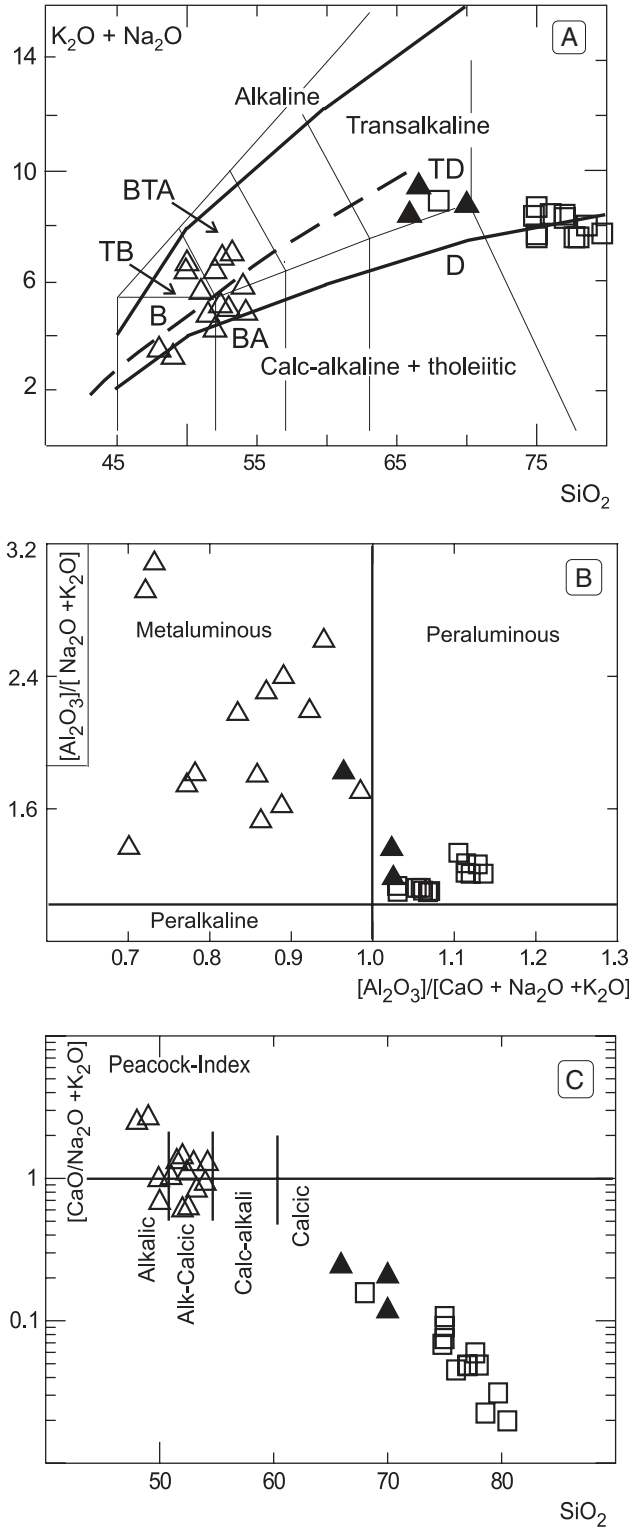

Fig. 3. Geochemical classification of the investigated rocks. (A) Total alkalis vs. silica diagram (Le Maitre, 1989), the dashed line is Irvine and Bar agar's divider between alkaline and subalkaline rocks, whereas the solid lines are Middlemost's dividers between alkaline, midalkaline and subalkaline fields (Middlemost, 1997). (B) A/NK vs. A/CNK Shand diagram; (C) peacock diagram after Brown (1981). Symbols: open triangles = Ghuweir mafics; solid triangles = Ghuweir rhyolites and rhyodacites; open squares = Feinan granites.

characterized by chondrite-normalized patterns with steep slopes from La to Sm [(La/Sm) $n = 3$–5.7] and flat ones from Gd to Lu [(Gd/Lu) $n = 0.9$–1.8; only one sample has a higher ratio up to 3.2], thereby contrasting with the regular slopes observed for GM patterns (see below). The flat HREE patterns rule out the involvement of garnet in the petrogenesis of these granites. Furthermore, the FG has a steadily increasing Eu depletion with simultaneous decrease in the total REE [Eu/Eu* = 0.07–0.53]. The GR rocks have REE patterns remarkably similar to that of the most primitive granite of the FG (Fig. 6B). They have [$\sum$REE = 186–220 ppm; (La/Lu)$n = 9.2$–11.8; (La/Sm)$n = 3.18$–3.59; (Gd/Lu)$n = 1.82$–2.19; and Eu/Eu* = 0.60–0.64]. The REE patterns of the GR suggest that the derivation of these rhyolites/rhyodacites from mafic melts similar to the GM via fractional crystallization must have been achieved through a different fractionation assemblage which gave rise to the intra-suite variation in the GM. In particular, the role of plagioclase fractionation is more obvious as reflected in the negative Eu anomaly of the rhyolites compared to the REE patterns of the GM. The REE patterns, however, taken with other evidence strongly argue for a genetic relationship with the FG.

The GM show a wide range of REE contents ($\sum$REE = 64–348 ppm), with (La/Lu)$n = 5.1$–15.4; all samples have a slightly negative Eu anomaly (Eu/Eu* = 0.78–0.97); and display a regular decrease of the slopes of REE patterns [(La/Sm)$n = 1.86$–3.05; (Gd/Lu)$n = 2.2$–3.5] (Fig. 6C). The LREE/HREE increases with increasing $\sum$REE and decreasing Mg#.

Primitive mantle-normalized plots (Sun and McDonough, 1989) of the FG, GR and GM are shown in Fig. 7A, B, and C. The FG show strongly negative anomalies at Ti, P, Sr, and Ba and a moderate negative anomaly at Nb. The GR shows the same, though not so strong, type of depletion as in the FG with the exception of Ba, which implies that the anomalies in the FG intensified as a result of fractional crystallization as it is apparent from the increasing depletion with decreasing Mg#. With the exception of the Nb anomaly, all other features are also typical of anorogenic granites. These geochemical signatures are similar to those displayed by post-collisional high-K granitoids from the Late Neoproterozoic of the Arabian-Nubian Shield and the East African Orogen and late Pan-African granitoids in general (e.g. Küster and Harms, 1999; Beyth et al., 1994; Hassanen, 1997; Liégeois et al., 1998). The patterns for the GM display moderate but distinct Nb and Th anomalies, which do not change much with differentiation. On the other hand, strontium shows a positive spike in the most primitive compositions (Mg# 61) and becomes progressively depleted in the more evolved compositions. P is slightly depleted in the primitive compositions and becomes progressively concentrated in the differentiated samples.

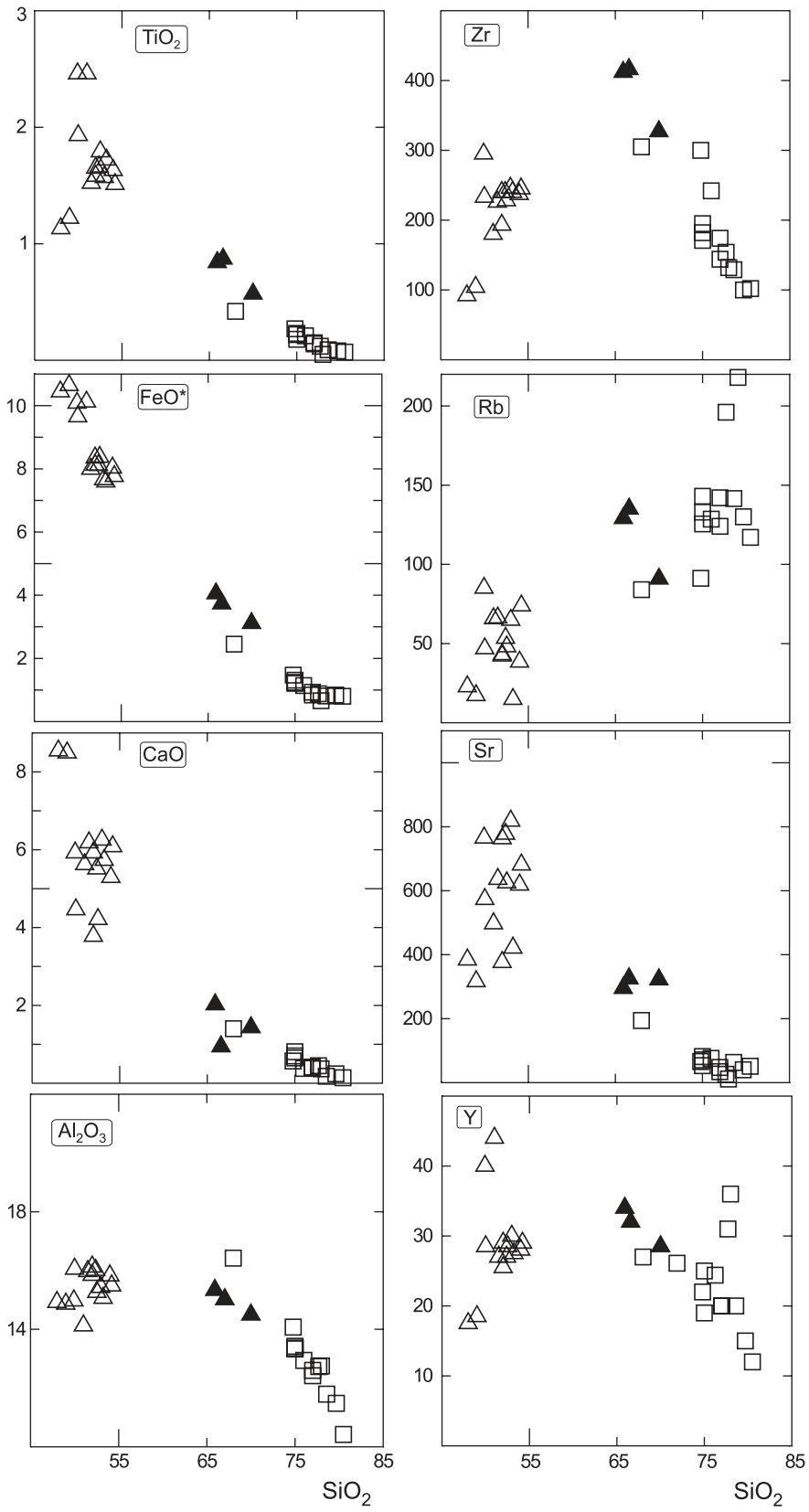

Fig. 4. SiO_2 Harker type variation plots. Symbols as in Fig. 3.

Please cite this article as: Jarrar, G., et al., Late Neoproterozoic A-type granites in the northernmost Arabian-Nubian Shield formed by fractionation of basaltic melts. Chemie der Erde (2006), doi:10.1016/j.chemer.2006.09.002

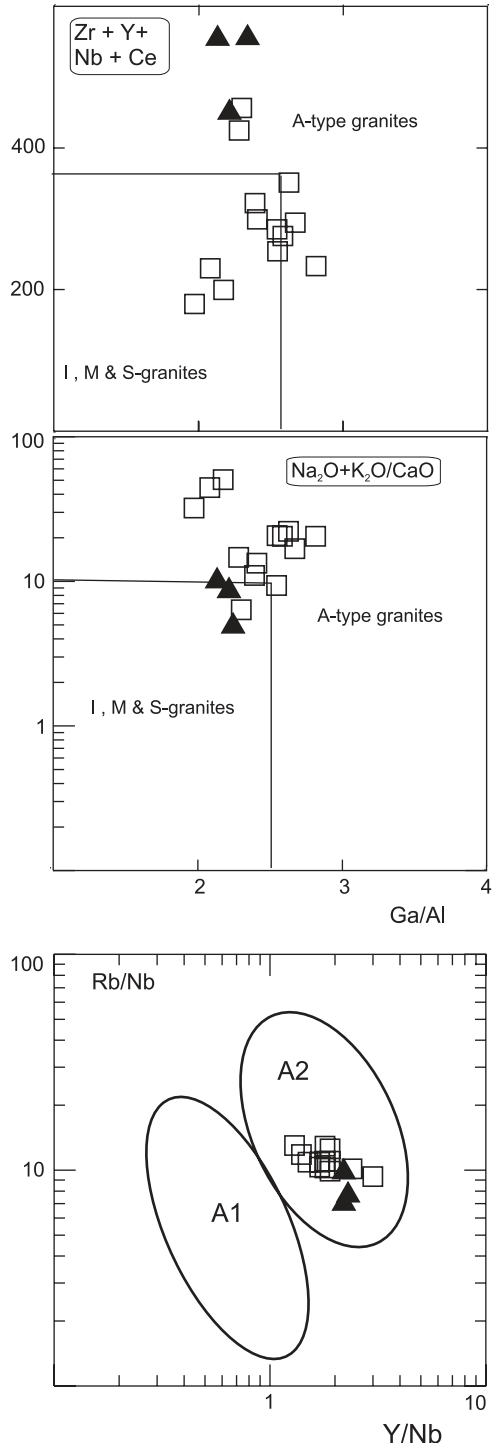

Fig. 5. Binary geochemical discrimination plots for A-type granites (Whalen et al., 1987; Eby, 1992).

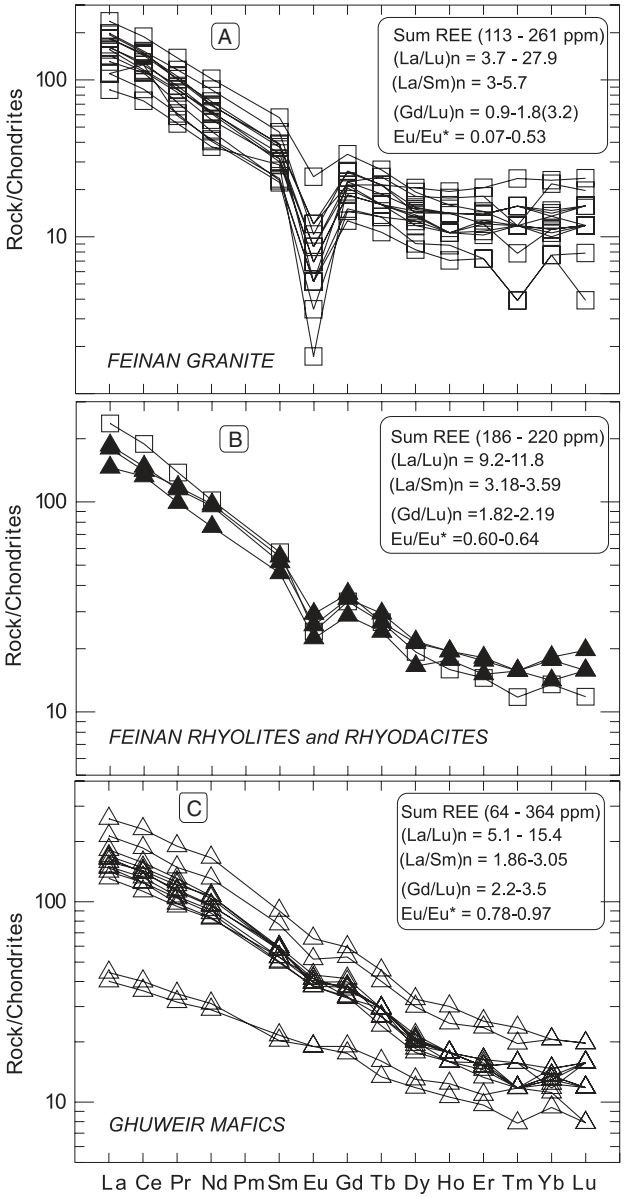

Fig. 6. Chondrite-normalized REE abundances for the investigated suite: (A) Feinan Granites (FG); (B) Ghuweir rhyolites and rhyodacites (GR) together with the least evolved Feinan Granite (GW-34;open squares); (C) Ghuweir mafics. Normalizing values of chondrites are from Sun and McDonough (1989).

The enrichment in phosphorous with differentiation is reflected in the enrichment of the REE (see petrogenesis). Slight Ti and Hf depletions are evident in the primitive compositions, which intensify upon differentiation.

7. Tectonic setting

The emplacement of the FGMS at approximately 560–570 Ma occurred during a period of extensive uplift and erosion of the upper crust which is manifested by the widespread occurrence of terrestrial sedimentary basins filled with abundant granitoid components (e.g. Saramuj Conglomerate in Jordan, Hammamat series in NE Desert of Egypt). There is strong evidence for extension dating back to as early as 600 Ma in

Please cite this article as: Jarrar, G., et al., Late Neoproterozoic A-type granites in the northernmost Arabian-Nubian Shield formed by fractionation of basaltic melts. Chemie der Erde (2006), doi:10.1016/j.chemer.2006.09.002

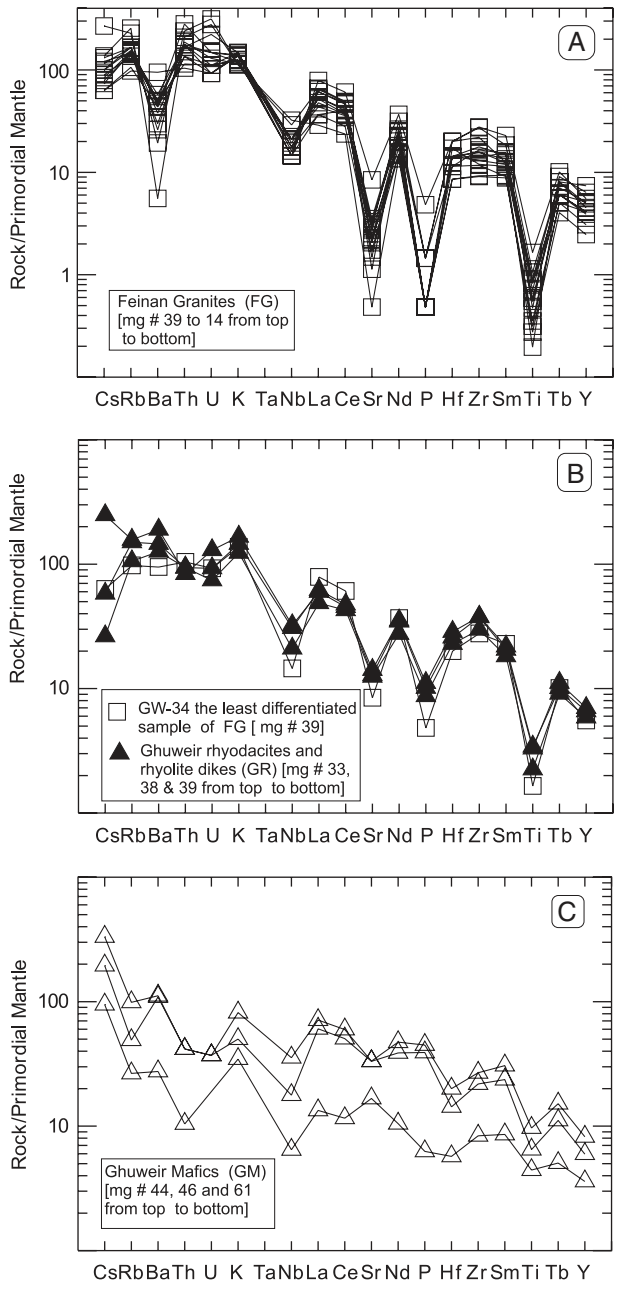

Fig. 7. Primitive mantle-normalized multi-element plots for: (A) Feinan Granites; (B) Ghuweir rhyolites and rhyodacites (GR) with the least evolved Feinan Granite (GW-34); (C) Three selected samples from the Ghuweir Mafics (GM). Normalizing values of primitive mantle are from Sun and McDonough (1989).

Southwest Jordan (Jarrar et al., 1993) NE desert of Egypt (Stern and Gottfried, 1986) and even 615 Ma in southern Israel (Beyth et al., 1994). The sediments of these fault-bounded basins are often intruded by the FGMS-like magmatic phases, i.e. Saramuj conglomerate (Jarrar et al., 1993) and the GM intrude the Saramuj-type sediments in Wadi Ghuweir (Fig. 1).

The FG and GR are plotted on Pearce et al. (1984) tectonic discrimination diagram Rb vs. (Y + Nb) (Fig. 8A). The investigated granites fall in the field of volcanic arc granites (VAG) very close to the within plate granites (WPG). The calc-alkaline granites of the Aqaba Complex (Ibrahim and McCourt, 1995), e.g. granitoids older than the Saramuj Conglomerate (>600 Ma) and the alkaline and peralkaline rhyolites exposed along the eastern rim of Wadi Araba (Araba complex, ~550 Ma; Jarrar, 1992; Jarrar et al., 1992) are plotted for the sake of comparison. The FGMS is transitional between true volcanic-arc tectonic environment and true within-plate environment. The GM plot in the field of within-plate lavas on the Zr/Y vs. Zr plot (Fig. 8B), and mainly in the overlapping field on the Nb vs. SiO_2 plot. Furthermore, the FG and GR plot in the overlapping field between the within plate and volcanic arc lavas on the Nb vs. SiO_2 diagram of Pearce and Gale (1977; Fig. 8C). Nevertheless, the granites of this suite fall within the fields assigned to A-type granites (Whalen et al., 1987) and post-collisional granites (Pearce, 1996). The fields occupied by the alkaline and peralkaline rhyolites of the Araba complex and the youngest mafic dike suite (Jarrar, 2001) are shown on the Nb–SiO_2 plot for comparison. Both suites are younger than the FGMS and represent truly within plate lavas.

8. Petrogenesis

8.1. The GMs

The GMs span a compositional range (SiO_2 48–54 wt %) and are characterized by high K_2O (0.75–2.48 wt%) and by relatively high TiO_2 (1.13–2.46 wt%) and P_2O_5 (0.13–1.35 wt%) contents. Furthermore, they are enriched in the incompatible trace elements (LILE, HFSE) but show a negative Nb anomaly and a Mg# ranging from 61 to 44.

Experimental work demonstrates that K_2O metasomatism of the mantle wedge overlying the subduction zone is capable of producing K-rich mantle phases like phlogopite or K-richterite (Schmidt, 1996). Turner et al. (1996) suggested a phlogopite-rich lithospheric mantle as a source for the post-collisional potassic magmas in Tibet.

Our model for the petrogenesis of the Feinan granite involves the generation of the GMs by batch modal partial melting of LILE- enriched, phlogopite-bearing lithospheric mantle which was modified by previous subduction during the main phase of the Pan-African Orogeny.

The mantle source composition is selected as a phlogopite-bearing spinel lherzolite with the following mineralogy: olivine: orthopyroxene: clinopyroxene:

Please cite this article as: Jarrar, G., et al., Late Neoproterozoic A-type granites in the northernmost Arabian-Nubian Shield formed by fractionation of basaltic melts. Chemie der Erde (2006), doi:10.1016/j.chemer.2006.09.002

spinel: phlogopite = 65:20:10:4:1. The element concentrations are taken as primitive mantle compositions (Sun and McDonough, 1989). Concentrations of LREE including Eu, in addition to Ba, Sr, Th, and U are set as twice primitive mantle while Rb and K are taken as triple the primitive mantle composition. A batch modal partial melting model was used (Rollinson, 1993). The input and output of the modeling process are given in Table 3A and Fig. 9. The composition of the melt with 5% and 10% partial melting along with the chemistry of the two most primitive samples of the GM are given. These two samples best approach primary mantle melt compositions. Inspection of the results show excellent agreement between the composition of the least evolved samples of the GMs (GW-23 and GW-22) and the $F = 10\%$ partial melt. Deviations from the model are expected due to the uncertainties in the choice of the distribution coefficients. It must also be borne in mind that the modeling of partial melting process using trace elements to suggest an approximate candidate for the source composition of a given igneous suite is based on several assumptions, which renders any derived model a probable but never a unique solution. On the basis of the above discussion, we conclude that the GM were derived by 10% partial melting of a phlogopite spinel lherzolite mantle source.

The drop in Mg# from 61 to 44 which is accompanied by a drastic decrease in Ni from 175 to 10 ppm; an increase in P_2O_5 (0.13–1.35 wt%); TiO_2 (1.22–2.48 wt%); REE (64–348 pmm); Zr (92–295 ppm) in addition to many other chemical characteristics (see Fig. 4) are not explicable by varying degrees of partial melting. Fractional crystallization must be called upon to account for these changes. Inspection of Figs. 4 and 10 suggest that the GM evolved by the fractionation of the three mineral assemblage olivine, clinopyroxene, and plagioclase. The high contents of REE in the most evolved samples can be attributed to the accumulation of apatite (see Fig. 10; the excellent correlation between total REE and the P_2O_5 contents).

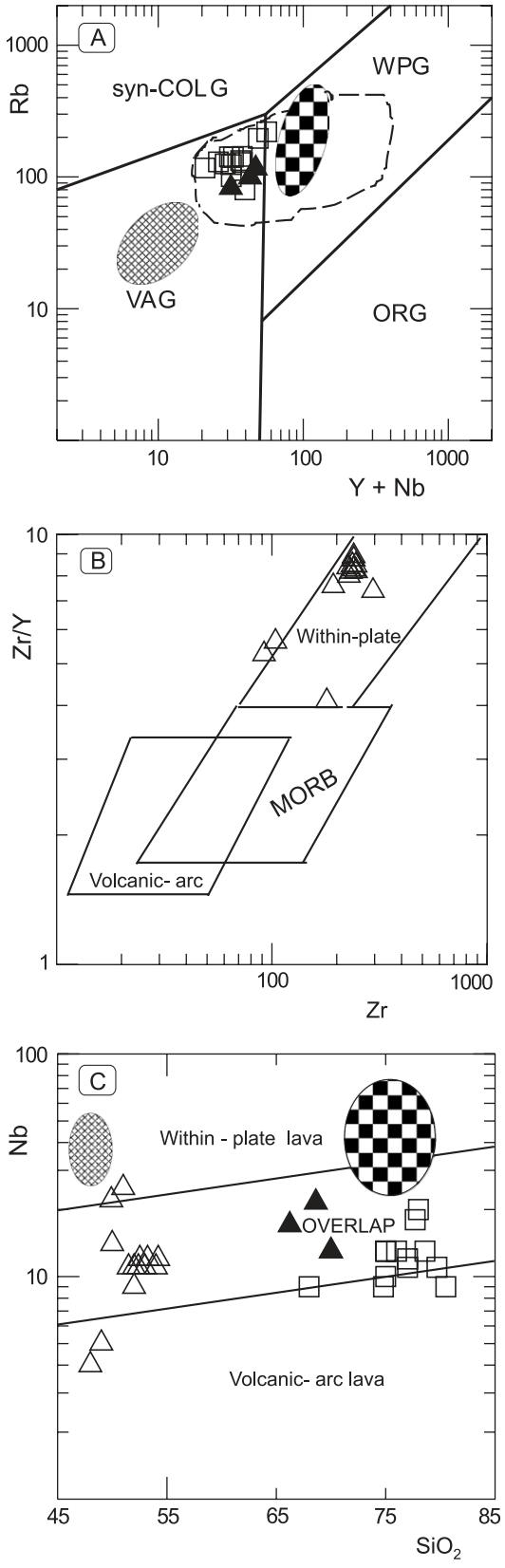

Fig. 8. Tectonic discrimination diagrams of the FGMS: squares = FG and triangles = GM in all plots; (A) Rb vs. (Y + Nb) after Pearce et al. (1984), the hatched area is for the calc-alkaline granite of the Aqaba complex (Ibrahim and McCourt, 1995) and the chess board symbols stand for the Aheimir Rhyolites (~550 Ma, Jarrar, 1992), and the dashed line is the field of post-collision granites (Pearce, 1996) and A-type granites (Whalen et al., 1987); (B) Zr/Y vs. Zr after Pearce and Norry (1979); (C) Nb vs. SiO_2 after Pearce and Gale (1977), the chess board symbols stand for the Aheimir Rhyolites and the hatched area for the youngest mafic dyke suite both part of the Araba complex.

8.2. The A-type granites (Ghuweir rhyolites/rhyodacites (GR) and the FGs)

Ratios of the highly incompatible elements are listed in Table 2. Most of these ratios, excluding Ba/La, are

Please cite this article as: Jarrar, G., et al., Late Neoproterozoic A-type granites in the northernmost Arabian-Nubian Shield formed by fractionation of basaltic melts. Chemie der Erde (2006), doi:10.1016/j.chemer.2006.09.002

Table 3. Rare earth and other trace element modeling of the partial melting and Rayleigh fractional crystallization processes which gave rise to the Feinan A-type granite and coeval Ghuweir Mafics

A. Partial melting of a phlogopite bearing spinel lherzolite to generate the Ghuweir Mafics (GM)							B. Fractional crystallization of the Ghuweir Mafics to produce the Ghuweir Rhyolites and rhyodacites (GR) and the Feinan Granites (FG)						C. Fractional crystallization within the Feinan granite suite				
	Source	*D*	*F* = 5%	*F* = 10%	GW-23 Mg# 61	GW-22 Mg# 59		*D**	GW-23	Calc[b]	Av GR	GW-34		*D***	GW-34	GW-26	Calc[c]
K[a]	750 ppm	0.03	0.83	0.52	1.05	0.82	K	0.14	1.05	3.76	4.4	4.18	Rb	0.68	84	130	124.5
Rb	1.905	0.03	15.9	9.9	22.8	17.9	Rb	0.05	22.8	94	118	84	Ba	1.71	717	287	300.0
Ba	13.978	0.02	191	115	208	235	Ba	0.03	208	890.3	1161	717	Sr	2.21	194	40	44.1
Sr	42.2	0.02	577.3	346	384	316	Sr	1.4	384	211.22	302	194	U	0.74	2.5	2.5	3.4
U	0.042	0.00	0.8	0.4	<0.5	<0.5	U	0.03	0.4	1.7	2.66	2.5	Th	0.86	10	13	11.8
Th	0.17	0.03	2.1	1.3	1	1	Th	0	1	4.42	8.9	11	Zr	0.48	305	100	80.0
Ti[a]	1205 pm	0.08	1.53	1.13	1.22	1.13							Hf	1.57	7	3	3.5
Zr	11.2	0.07	98.2	69.7	92	104	Zr	0.13	92	336	385	305	Nb	0.61	9	11	14.5
Hf	0.309	0.05	3.1	2.1	2	3	Hf	0.09	2	7.76	9	7	Y	1.51	27	15	14.5
Nb	0.713	0.10	5	3.8	4	5	Nb	0.24	5	15.5	17.3	9	La	1.79	56	26	21.2
Y	4.55	0.14	25.8	20.7	17.5	18.5	Y	0.62	17.5	30.75	31.5	27	Ce	1.57	115.5	53.5	57.6
La	1.374	0.02	10.7	6.1	9.5	10.5	La	0.05	9.5	39.2	40.3	56	Nd	1.73	47.5	19	19.4
Ce	3.55	0.03	24.3	14.6	22	24.5	Ce	0.05	22	91.13	85.7	115.5	Sm	1.68	8.8	3.4	3.8
Pr	0.552	0.07	4.8	3.4	3	3.3	Pr	0.03	3	12.8	10.5	13.1	Eu	2.66	1.4	0.2	0.2
Nd	2.708	0.08	15.1	9.8	13.5	14.5	Nd	0.16	13.5	47.55	41.8	47.5	Gd	1.69	6.9	3	3.0
Sm	0.888	0.07	4.0	2.8	3.3	3.1	Sm	0.28	3.3	9.59	7.77	8.8	Dy	1.71	4.9	2.3	2.1
Eu	0.168	0.07	1.5	1.1	1.1	1.1	Eu	0.73	1.1	1.66	1.5	1.4	Er	1.61	2.4	1.2	1.1
Gd	0.596	0.09	4.6	3.4	3.6	3.9	Gd	0.35	3.6	9.43	6.8	6.9	Yb	1.37	2.3	1.3	1.5
Tb	0.108	0.06	2.7	2.2	0.5	0.6	Tb	0.32	0.5	1.38	1	1	Lu	1.27	0.3	0.2	0.2
Dy	0.737	0.10	4.9	3.8	3	3.3	Dy	0.57	3	5.66	5.03	4.9	V	2.69	20	2.5	2.5
Ho	0.164	0.13	0.9	0.7	0.6	0.7	Ho	0.47	0.6	1.33	1.07	0.9	Ni	1.35	10	5	6.5
Er	0.48	0.12	2.9	2.3	1.6	1.8	Er	0.42	1.6	3.8	2.8	2.4	Ga	1.37	20	12	12.8
Tm	0.074	0.12	0.5	0.4	0.2	0.3	Trn	0.27	0.2	0.6	0.4	0.3					
Yb	0.493	0.14	2.3	1.9	1.6	1.9	Yb	0.42	1.6	3.8	2.83	2.3					
Lu	0.074	0.15	0. 40	0.30	0.20	0.20	Lu	0.67	0.2	0.33	0.45	0.3					
Ni	1890	11.9	183	193	175 1	170	V	2.7	185	14.73	45	20					
Cr	2935	7.53	364	382	274	274	Ni	3.33	175	5.44	6.7	10					
V	164	0.30	521	467	185	190	Cr	4.56	274	1.35	<68	<68					
P[a]	95 ppm	0.03	0.51	0.31	0.13	0.15	P	0.01	0.13	0.57	0.2	0.1					
Sn	0.17	0.09	1.3	0.9	1	<1	Ga	0.96	18	19.11	17.6	20					
Ga	3.9	0.24	14.2	12.5	18	19											

The partition coefficients used for the calculation of the bulk distribution coefficients (D) where selected from GERM (geochemical earth reference model; http://www.earthref.org/GERM/) and from Rollinson (1993). The data in this table is shown in Fig. 9.

Source is taken as phlogopite bearing spinel lherzolite with the following mineralogy: oliv:opx:cpx:spl:phlog = 65:10:20:4:1; the element concentrations are taken as primitive mantle compositions (Sun and McDonough, 1989). The REE including Eu, Ba, Sr, Th, and U are taken twice PM while the Rb and K are taken as triple the PM compositions.

D: Bulk distribution coefficient calculated using Kd values compiled in GERM and the mineralogy of the source given above.

*D**: Bulk distribution coefficient calculated for the fractionated mineral assemblage: olivine:plagioclase:pyroxene:magnetite = 16:26:47:11.

The separated mineral phases are amphibole:Na-feldspar:K-feldspar: magnetite:apatite = 9.31:63.5:24.1:15:0.6 in addition to 0.1 wt% of zircon, titanite and allanite.

*D*** is the bulk distribution coefficient for the various elements calculated from the listed Kd values.

GW-34 and GW-26 are the least and the most fractionated granitic samples, respectively.

[a]The modeled concentrations are in wt% as oxides.

[b]The calculated concentrations in the residual melt after fractionating the above mineral assemblage (*F* = 0.225 as deduced from major element modeling).

[c]Calculated melt composition after fractionating 70 wt% of the granitic magma (GW-34).

identical for the GM and GR which argues for a fractional crystallization relationship between the two rock suites. These ratios, in particular the K/Ba, Ba/La, and Rb/Sr, are, however, different for the FG. This can be attributed to the fact that Sr and Ba change from incompatible behavior in the GM to compatible behavior in the FG magmas while Rb and K remain strongly incompatible. It should however be emphasized that these ratios vary widely in the GM and FG, which can be attributed to the extensive fractional crystallization as will become evident from major elements modeling.

To test our assumption regarding the derivation of GR via fractional crystallization of the GM and subsequently the fractionation of the GR and the most primitive FG samples (represented by sample GW-34) to

Please cite this article as: Jarrar, G., et al., Late Neoproterozoic A-type granites in the northernmost Arabian-Nubian Shield formed by fractionation of basaltic melts. Chemie der Erde (2006), doi:10.1016/j.chemer.2006.09.002

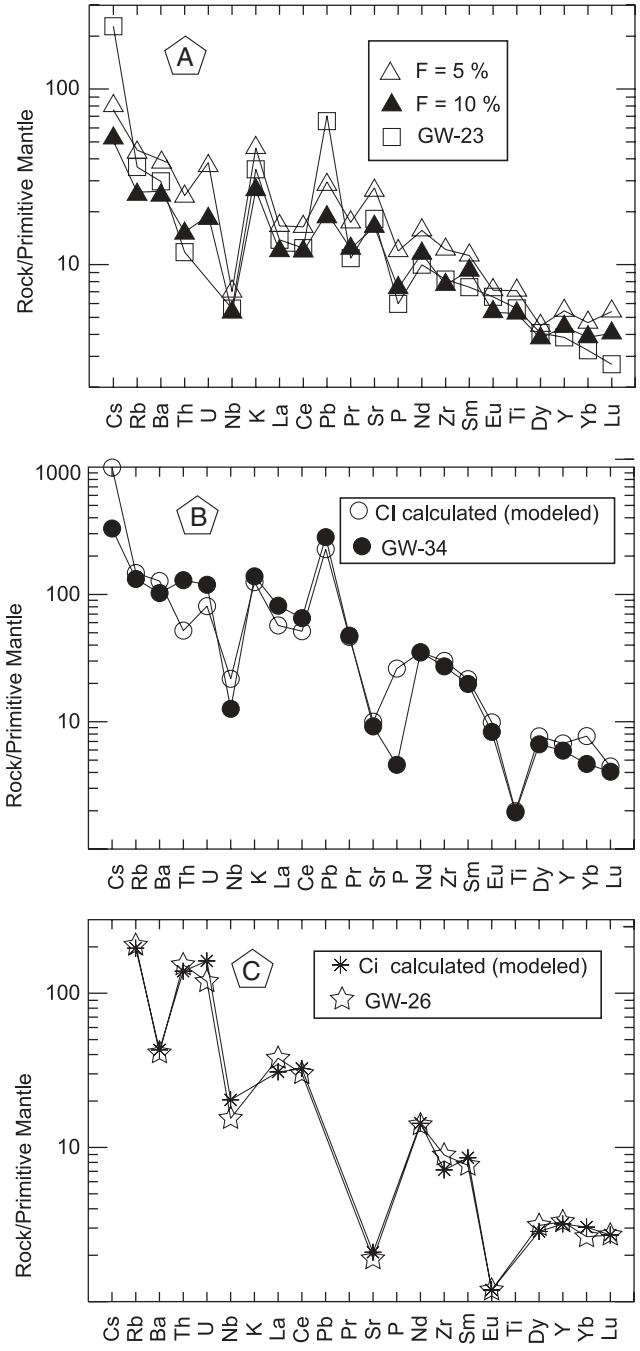

Fig. 9. A comparison between observed and modeled compositions shown in Table 3. The normalization factors are after Sun and McDonough (1989).

give rise to the whole spectrum of the Feinan granites, we used major elements least squares modeling utilizing the program of Stormer and Nicholls (1978). The results of major elements modeling are listed in Table 4. The fractional crystallization of a four mineral assemblage (olivine:pyroxene:plagioclase:magnetite = 12.37:19.13:36.63:8.31; $F = 0.225$) would be necessary to produce the most primitive of the A-type granites (Table 4A), i.e. the most primitive sample of the FG (GW-34; Mg# = 39). To test the validity of this model the trace elements modeling using the Rayleigh fractional crystallization described above was applied (Table 3B). The calculated melt composition (Calc.**) is compared with the composition of the most primitive sample of the Feinan Granite (GW-34) and the average GR samples. There is a good agreement between the calculated melt and the observed compositions (Fig. 9B), which supports the hypothesis that the A-type granitic melt was produced by extensive fractional crystallization of a mantle derived mafic magma (GMs). Inspection of Figs. 4 and 10 reveals that the Feinan A-type granites and the Ghuweir Rhyolites and rhyodacites suffered extensive fractional crystallization of K- and Na-feldspars in addition to amphibole and small amounts of the accessory mineral phases, magnetite, zircon, apatite, and allanite. Again we employed least squares modeling of major elements and found that the most evolved granitic sample (GW-25 or GW-26; Mg# 14 and 10, respectively) can be produced from the most primitive granite (GW-34; Mg# = 39) by the separation of the mineral assemblage (amphibole:Na-feldspar:K-feldspar:magnetite:apatite = 6.42:43.78:16.61:1.48:0.43) (Table 4B).

This model was tested by the Rayleigh fractional crystallization on the trace elements (Table 3C). Reasonably good agreement can be seen between the calculated melt composition and the observed melt compositions (GW-26, the most differentiated sample of the Feinan A-type granite; Fig. 9C) which lends support for the usefulness the major elements modeling.

9. Regional correlation

Chondrite-normalized plots were prepared (Fig. 11) for the GMs and the coeval mafic rocks in the Western Desert of Egypt (Bir Safsaf), North Eastern Desert of Egypt and in the area of Timna on the western shoulder of Wadi Araba. Although a general similarity of the patterns is obvious which reflect the generally similar tectonic setting of these rocks, the patterns of Timna monzodiorite and andesite, the Bir Safsaf and the Dokhan andesites are steeper, i.e. more enriched in LREE than the GMs. This becomes clear when the primitive compositions are compared. Differences in the REE patterns probably reflect different sources.

The Feinan area has been and still is considered as the eastern continuation of the Timna area mainly on the basis of the correlating the strata bound copper mineralization in both districts. It is believed that both copper districts were originally a contiguous complex, which became separated by the lateral movement along the Jordan-Dead Sea Transform for about 100 km (e.g.

Please cite this article as: Jarrar, G., et al., Late Neoproterozoic A-type granites in the northernmost Arabian-Nubian Shield formed by fractionation of basaltic melts. Chemie der Erde (2006), doi:10.1016/j.chemer.2006.09.002

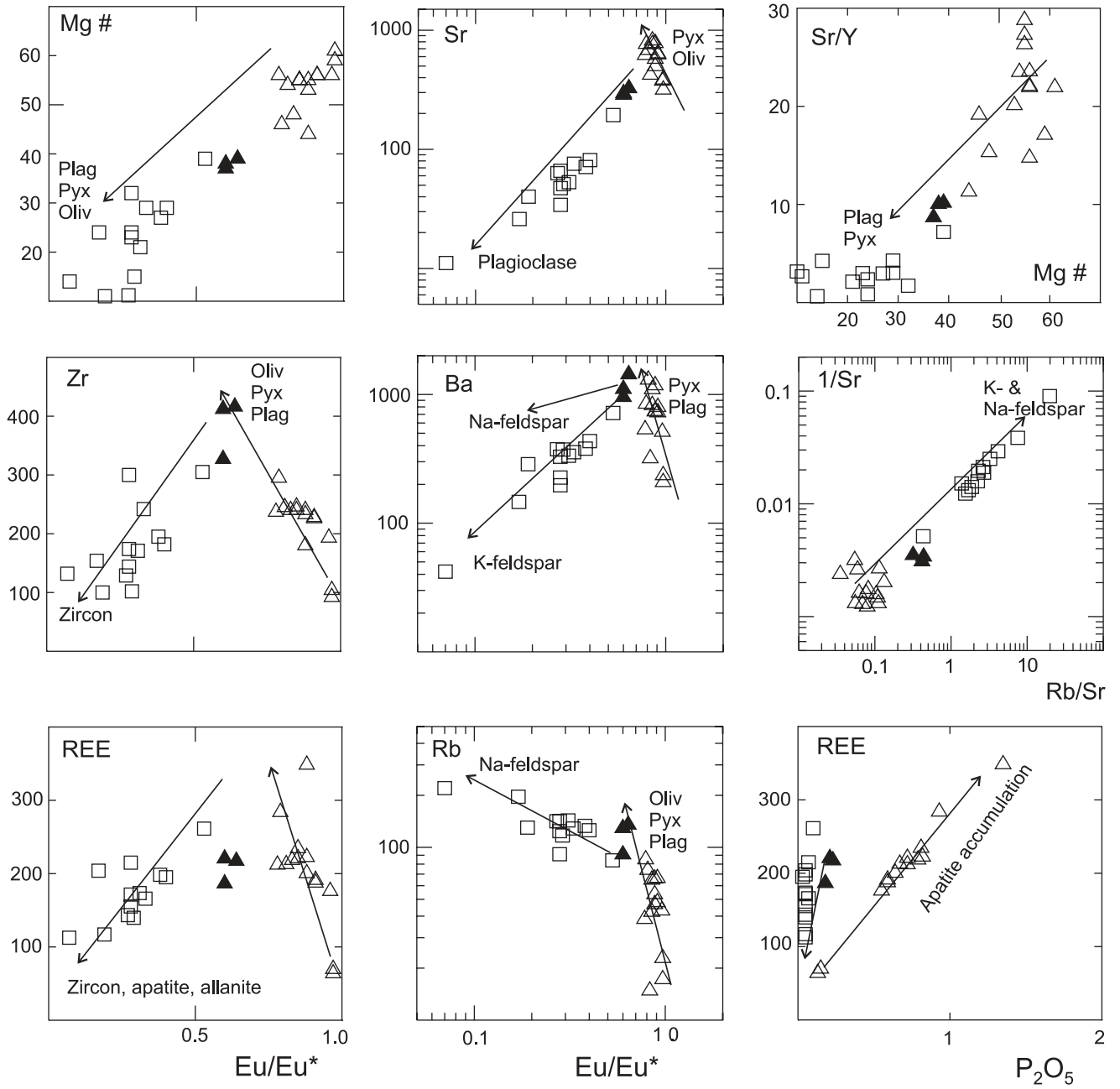

Fig. 10. Selected binary plots to show the chemical effects of fractionation of mineral phases in the evolution of the FGMS. The arrows indicate the compositional changes due to the fractionation of minerals; only in one case (REE vs. P_2O_5 plot) it shows the role of apatite accumulation in the magma in the increase of REE abundances. Abbreviations used for the minerals are similar to those in Table 3. The symbols as in Fig. 3.

Freund et al., 1970; Zak and Freund, 1981). Opponents to the large-scale strike slip movement along the Dead Sea Transform explain the mismatch of the sedimentary sequences by lateral facies change along the palaeo-shorelines (e.g. Bender, 1982). When the age difference between the investigated FGMS (560–570 Ma) and the Timna Igneous Complex (610–625 Ma; Beyth et al., 1994) is taken into account together with differences in petrography and geochemistry we can claim that our results do not support the assumption that the Timna and Feinan areas once belonged to a contiguous igneous complex.

10. Conclusions

The Ghuweir Feinan Magmatic Suite comprises two end members: a felsic end member, the Feinan granite and the Ghuweir rhyolites and rhyodacite dikes, which

Please cite this article as: Jarrar, G., et al., Late Neoproterozoic A-type granites in the northernmost Arabian-Nubian Shield formed by fractionation of basaltic melts. Chemie der Erde (2006), doi:10.1016/j.chemer.2006.09.002

Table 4. Major elements modeling of fractional crystallization processes

	Parent	Daughter	Assemblage fractionated			
	GW-23	GW-34	OLV	CPX	PLAG	MT
A. Fractionation from the most primitive GM composition (GW-23, Mg# = 61) to most primitive FG composition (GW-34, Mg# = 39)						
SiO_2	49.60	68.81	40.24	49.30	53.29	0.09
TiO_2	1.22	0.43	0.00	1.67	0.04	0.00
$A1_2O_3$	15.42	16.61	0.00	4.60	29.17	2.25
FeO_t	11.99	2.75	12.30	8.55	0.25	93.13
MgO	9.23	0.87	47.02	14.69	0.07	4.53
CaO	8.82	1.42	0.44	20.72	12.16	0.00
Na_2O	2.50	4.78	0.00	0.45	4.74	0.00
K_2O	1.09	4.23	0.00	0.02	0.28	0.00
P_2O_5	0.13	0.10	0.00	0.00	0.00	0.00
Crystals removed in wt%			12.26	20.33	36.18	8.73
$R^2 = 0.71$; $F = 22.5$ wt%			CUM = 77.5 wt%			

	Parent	Daughter	Assemblage fractionated				
	GW-34	GW-26	Na-FLD	K-FLD	AMPH	AP	MT
B. Fractionation from the least evolved to the most evolved granite (GW-34 to GW-26, Mg# = 10)							
SiO_2	68.81	79.54	68.51	64.05	49.77	0.63	0.00
TiO_2	0.43	0.08	0.00	0.00	0.69	0.00	3.05
$A1_2O_3$	16.62	11.45	20.60	18.00	7.84	0.00	1.47
FeOt	2.75	0.93	0.09	0.26	14.63	0.00	90.51
MgO	0.87	0.06	0.00	0.00	14.58	0.00	4.97
CaO	1.42	0.24	0.34	0.00	11.06	57.02	0.00
Na_2O	4.78	3.57	9.54	0.87	1.13	0.53	0.00
K_2O	4.22	4.12	0.92	16.82	0.30	0.00	0.00
P_2O_5	0.10	0.01	0.00	0.00	0.00	41.82	0.00
Crystals removed in wt%			43.78	16.61	6.42	0.43	1.48
$R^2 = 1.08$, $F = 31.08$ wt%			CUM = 68.92 wt%				

The program XLFRAC (Stormer and Nicholls, 1978) was used for the least squares modeling. The chemical compositions of the minerals used in the modeling were taken from Jarrar (1998), Jarrar et al. (1993), and Deer et al. (1992).
R^2 = Residual sum of squares, OLV = olivine; CPX = clinopyroxene, PLAG = plagioclase, FLD = Feldspar, AMPH = amphibole, MT = magnetite, F = fraction of magma remaining; CUM = the total amount of fractionated mineral assemblage; FeO_t = total iron as FeO

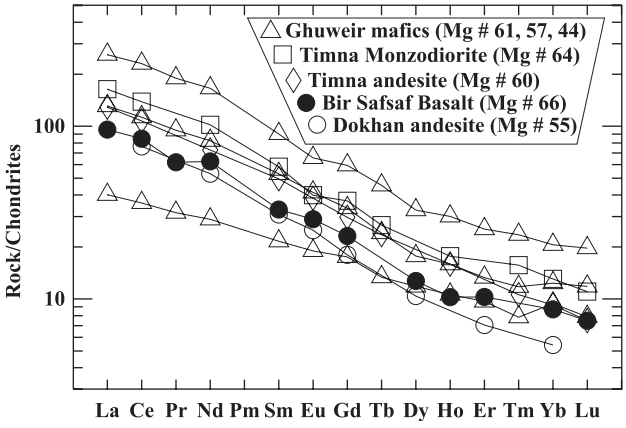

Fig. 11. Chondrite-normalized patterns for the Ghuweir Mafics and the equivalent rocks from the adjacent countries.

are classified as A-type granites; and the GMs which are comagmatic (coeval) with the Feinan granites. This suite has been selected to investigate the genetic relationship between A-type granitic magmas and their mafic coeval magmas. For this purpose the field relationships, the petrography, geochemistry and geochronology of this suite have been investigated in some detail. The conclusions drawn from this study regarding this suite and other similar suites can be summarized in the following points:

1. Geochemical, isotopic and age constraints support the hypothesis that the FGMS comprises a comagmatic suite with mafic and granitic end members, associated in space and time. This suite formed between 556 and 572 Ma ago according to Rb–Sr

whole-rock dating and has low Sr and high Nd initial ratios that preclude significant crustal contribution in the magma genesis.
2. The FGMS forms a discontinuous series in terms of silica contents (a gap at SiO_2 55–65). It has a transalkaline to alkaline character; belongs to the medium to high K series and even extends to the shoshonitic series; it ranges from metaluminous to mildly peraluminous and belongs to the alkali and alkali-calcic series.
3. The Feinan granites and the Ghuweir rhyolites and rhyodacites are classified as A-type granites and belong to group A2 of Eby (1992). Furthermore, these granites plot close to the transition between volcanic arc granites and true within plate granites in the field of post-collision granites and as such they represent a transition in the tectonic style from collision to true extension and rift-related magmatism.
4. The GMs are enriched in LILE and HFSE and plot either in the field of within plate basalts or in the overlapping area between volcanic arc and true within-plate environment. Therefore, they indicate the same tectonic setting as the Feinan A-type granites.
5. The GMs were derived from a subduction modified lithospheric mantle by 10% batch modal partial melting of a phlogopite-bearing spinel lherzolite. The intra-suite geochemical variations can be ascribed to fractional crystallization of the assemblage olivine, pyroxene, and plagioclase. The accumulation of apatite in the most evolved samples is responsible for the high concentrations of REE.
6. The Feinan granites and the Ghuweir rhyolites and rhyodacites were modeled to have been derived from the mafic magma by fractional crystallization 77.5% of the original magma to the mineral assemblage olivine:pyroxene:plagioclase:magnetite. The intra-suite geochemical variations in the Feinan A-type granites are due to the fractional crystallization or accumulation of the mineral phases: amphibole + Na and K-feldspar + apatite + magnetite + zircon + allanite.
7. Our results do not support the assumption that the Feinan and Timna areas once formed a contiguous igneous complex.

Acknowledgements

The sabbatical leave granted by the University of Jordan to the first author is highly appreciated. This work was partially carried out while the first author was at the Geosciences Department, University of Texas at Dallas, USA as a Fulbright Fellow. The field work of this project and PC facilities were provided by Deanship of Academic Research, University of Jordan. The authors are grateful to an anonymous reviewer for his critical remarks that greatly helped to improve the manuscript.

References

Al-Bakri, N.M., 1990. Geochemistry and petrography of the Feinan porphyrite stock, Central Wadi Araba, Jordan. Unpublished M.Sc. Thesis, University of Jordan, Amman, Jordan.

Basta, E.Z., Abdel Kader, Z.M., Sunna, B.F., 1982. Geology and petrochemical characteristics of the Ghuweir Volcanics, Wadi El-Ghuweir Feinan district, Wadi Araba, Jordan. In: Abed, A., et al. (Ed.), Proceedings of the 1st Jordan Geological Conference, Amman, Jordan, pp. 297–338.

Bender, F., 1982. On the evolution of the Wadi Araba-Jordan Rift. Geol. Jb. B 45, 3–20.

Bentor, Y.K., 1985. The crustal evolution of the Arabo-Nubian massif with special reference to Sinai Peninsula. Precamb. Res. 28, 1–74.

Beyth, M., Stern, R.J., Altherr, R., Kröner, A., 1994. The late Precambrian Timna igneous complex, Southern Israel: evidence for comagmatic-type sanukitoid monzodiorite and alkali granite magma. Lithos 31, 103–124.

Brook, M., Ibrahim, K.M., McCourt, W.J., 1990. New geochronological data from the Arabian Shield area of southwest Jordan. In: Proceedings of the 3rd Jordanian Geological. Conference, Amman, Jordan, pp. 361–394.

Brown, G.C., 1981. Space and time in granite plutonism. Philos. Trans. R. Soc. London Ser. A 301, 321–336.

Collins, W.J., Beams, D.S., White, A.J.R., Chappell, B.W., 1982. Nature and origin of A-type granites with particular reference to southeastern Australia. Contrib. Mineral Petrol. 80, 189–200.

Creaser, R.A., Price, R.C., Wormald, R.J., 1991. A-type granites revisited: assessment of residual-source model. Geology 19, 163–166.

Eby, N.G., 1992. Chemical subdivision of the A-type granitoids: petrogenetic and tectonic implications. Geology 20, 641–644.

Freund, R., Garfunkel, Z., Zak, I., Goldberg, M., Weissbord, T., Derin, B., 1970. The shear along the Dead Sea rift. Philos. Trans. R. Soc. London 267A, 107–130.

Greiling, R.O., Abdeen, M.M., Dardier, A.A., AL-Akhal, H., EL-Ramly, M.F., Kamal-El Din, G.M., Osman, A.F., Rashwan, A.A., Rice, A.A., Sadek, M.F., 1994. A structural synthesis of the Proterozoic Arabian-Nubian Shield in Egypt. Geol. Rundsch. 83, 484–501.

Hadley, D.G., Schmidt, D.L., 1980. Sedimentary rocks and basins of the Arabian Shield and their evolution. In: Cooray, P.G., Tahoun, S.A., (Eds.), Evolution and Mineralization of the Arabian Nubian Shield. Institute of Applied Geology Jeddah Bulletin, vol. 3, pp. 25–50.

Hassanen, M.A., 1997. Post-collision, A-type granites of Homrit Waggat Complex, Egypt: petrological and geochemical constraints on its origin. Precamb. Res. 82, 211–236.

Please cite this article as: Jarrar, G., et al., Late Neoproterozoic A-type granites in the northernmost Arabian-Nubian Shield formed by fractionation of basaltic melts. Chemie der Erde (2006), doi:10.1016/j.chemer.2006.09.002

Ibrahim, K.M., McCourt, W.J., 1995. Neoproterozoic granitic magmatism and tectonic evolution of the northern Arabian Shield: evidence from Southwest Jordan. J. Afr. Earth Sci. 20, 103–118.

Irvine, T.N., Baragar, W.R.A., 1971. A guide to the chemical classification of the common volcanic rocks. Can. J. Earth Sci. 8, 523–548.

Jarrar, G.H., 1985. Late Proterozoic crustal evolution of the Arabian-Nubian Shield in the Wadi Araba area, SW-Jordan. Geol. Jb B 61, 3–87.

Jarrar, G.H., 1992. Geochemistry and petrogenesis of an alkali-feldspar rhyolite suite from Wadi Museimir, Central Wadi Araba, Jordan. Chem. Erde 52, 301–312.

Jarrar, G.H., 1998. Mineral chemistry in dioritic hornblendites from Wadi Araba, SW Jordan. J. Afr. Earth Sci. 26, 285–295.

Jarrar, G.H., 2001. The youngest Neoproterozoic mafic dyke suite in the Arabian Shield: mildly alkaline dolerites from South Jordan – their geochemistry and petrogenesis. Geol. Mag. 138, 309–323.

Jarrar, G.H., Wachendorf, H., Saffarini, G., 1992. A late Proterozoic bimodal volcanic/subvolcanic suite from Wadi Araba, Southwest Jordan. Precamb. Res. 56, 51–72.

Jarrar, G.H., Wachendorf, H., Zachmann, D., 1993. A Pan-African pluton intruding the Saramuj Conglomerate, South-west Jordan. Geol. Rundsch. 82, 121–135.

King, P.L., White, A.J.R., Chappell, B.W., Allen, M.C., 1997. Characterisation and origin of aluminous A-type granites from the Lachlan Fold Belt South-eastern Australia. J. Petrol. 38, 371–391.

Küster, D., Harms, U., 1999. Post-collisional potassic granitoids from the southern and north-western parts of the Late Neoproterozoic East African Orogen: a review. Lithos 45, 177–195.

Landenberger, B., Collins, W.J., 1996. Derivation of A-type granites from dehydrated charnockitic lower crust: evidence from the Chaelundi complex, eastern Australia. J. Petrol. 37, 145–170.

Le Maitre, R.W., 1989. A Classification of Igneous Rocks and Glossary of Terms. Recommendations of the IUGS Subcommission on the Systematic of Igneous Rocks. Blackwell, Oxford.

Lenz, H., Bender, F., Besang, C., Harre, W., Kreuzer, H., Müller, P., Wendt, I., 1972. The age of the early tectonic events in the zone of Jordan geosuture based on radiometric data. 24th International Geological Congress Section 3, pp. 371–379.

Liégeois, J.P., Naves, J., Hertogen, J., Black, R., 1998. Contrasting origin of post-collisional high-K calc-alkaline and shoshonitic versus alkaline and peralkaline granitoids. The use of sliding normalisation. Lithos 45, 1–28.

Ludwig, K.R., 2003. Isoplot 3: a geochronological toolkit for Microsoft Excel. Berkeley Geochronology Centre Special Publication No. 4, pp. 1–71.

McDonald, G.A., Katsura, T., 1964. Chemical composition of Hawaiian lavas. J. Petrol. 5, 83–133.

Maniar, P.D., Piccoli, P.M., 1989. Tectonic discrimination of granitoids. Geol. Soc. Am. Bull. 101, 635–643.

Middlemost, E.A.K., 1997. Magmas, Rocks and Planetary Development. Longman, Harlow, 229pp.

Miyashiro, A., 1978. Nature of alkalic volcanic rocks series. Contrib. Mineral. Petrol. 66, 91–104.

Pearce, J.A., Gale, G.H., 1977. Identification of ore deposition environment from trace elements geochemistry of associated igneous host rocks. In: Volcanic Process in Ore Genesis. Geological Society of London Special Publication, vol. 7, pp. 14–24.

Pearce, J.A., Harris, N.B., Tindle, A.G., 1984. Trace elements discrimination diagrams for the tectonic interpretation of granitic rocks. J. Petrol. 25, 956–983.

Pearce, J.A., Norry, M.J., 1979. Petrogenetic implications of Ti, Zr, Y, and Nb variations in volcanic rocks. Contrib. Mineral Petrol. 69, 33–47.

Pearce, J.A., 1996. Sources and settings of granitic rocks. Episodes 19, 120–125.

Rickwood, P.C., 1989. Boundary lines within petrologic diagrams which use oxides of major and minor elements. Lithos 22, 247–263.

Rollinson, H., 1993. Using Geochemical Data: Evaluation, Presentation, Interpretation. Longman Group, UK, 352pp.

Schmidt, M.W., 1996. Experimental constraints on recycling of potassium from subducted oceanic crust. Science 272, 1927–1930.

Stern, R.J., Gottfried, D., 1986. Petrogenesis of a Late Precambrian (575–600 Ma) bimodal suite in Northeast Africa. Contrib. Mineral Petrol. 92, 492–501.

Stern, R.J., Kröner, A., Bender, R., Reischmann, T., Dawoud, A.S., 1994. Precambrian basement around Wadi Halfa, Sudan: a new perspective on the evolution of the East African Craton. Geol. Rundsch. 83, 564–577.

Stoesser, D.B., Camp, V.E., 1985. Pan-African microplate accretion of the Arabian Shield. Bull. Geol. Soc. Am. 96, 817–826.

Stormer, J.C., Nicholls, J., 1978. XLFRAC: a program for the interactive testing of magmatic differentiation models. Comput. Geosci. 4, 143–159.

Sun, S-S., McDonough, W.F., 1989. Chemical and isotopic systematics of the oceanic basalts: implications for mantle composition and processes. In: Saunder, A.D., Norry, M.J. (Eds.), Magmatism in the Oceanic Basins. Geological Society London, London pp. 313–345.

Sylvester, P.J., 1989. Post-collisional alkaline granites. J. Geol. 97, 261–280.

Turner, S.P., Foden, J.D., Morrison, R.S., 1992. Derivation of some A-type magmas by fractionation of basaltic magma: An example from the Padthaway Ridge, South Australia. Lithos 28, 151–179.

Turner, S., Arnaud, N., Liu, J., Rogers, N., Hawkesworth, C., Harris, N., Kelly, S., Van Calsteren, P., Deng, W., 1996. Post-collision, shoshonitic volcanism on the Tibetian Plateau: implications for the convective thinning of the lithosphere and the source of ocean island basalts. J. Petrol. 37, 45–71.

Whalen, J.B., Currie, K.L., Chappell, B.W., 1987. A-type granites: geochemical characteristics, discrimination and petrogenesis. Contrib. Mineral Petrol. 95, 407–419.

Willis, K.M., Stern, R.J., Clauer, N., 1988. Age and geochemistry of the Precambrian sediments of the Hammamat series from the NE Desert of Egypt. Precamb. Res. 42, 173–187.

Zak, I., Freund, R., 1981. Asymmetry and basin migration in the Dead Sea Rift. Tectonophysics 80, 27–38.

Please cite this article as: Jarrar, G., et al., Late Neoproterozoic A-type granites in the northernmost Arabian-Nubian Shield formed by fractionation of basaltic melts. Chemie der Erde (2006), doi:10.1016/j.chemer.2006.09.002